

# Satellite Kinematics I: A New Method to Constrain the Halo Mass-Luminosity Relation of Central Galaxies

Surhud More<sup>\*</sup>, Frank C. van den Bosch, Marcello Cacciato

*Max Planck Institute for Astronomy, Königstuhl 17, D-69117, Heidelberg, Germany.*

## ABSTRACT

Satellite kinematics can be used to probe the masses of dark matter haloes of central galaxies. In order to measure the kinematics with sufficient signal-to-noise, one uses the satellite galaxies of a large number of central galaxies stacked according to similar properties (e.g., luminosity). However, in general the relation between the luminosity of a central galaxy and the mass of its host halo will have non-zero scatter. Consequently, this stacking results in combining the kinematics of satellite galaxies in haloes of different masses, which complicates the interpretation of the data. In this paper we present an analytical framework to model satellite kinematics, properly accounting for this scatter and for various selection effects. We show that in the presence of scatter in the halo mass-luminosity relation, the commonly used velocity dispersion of satellite galaxies can not be used to infer a unique halo mass-luminosity relation. In particular, we demonstrate that there is a degeneracy between the mean and the scatter of the halo mass-luminosity relation. We present a new technique that can break this degeneracy, and which involves measuring the velocity dispersions using two different weighting schemes: host-weighting (each central galaxy gets the same weight) and satellite-weighting (each central galaxy gets a weight proportional to its number of satellites). The ratio between the velocity dispersions obtained using these two weighting schemes is a strong function of the scatter in the halo mass-luminosity relation, and can thus be used to infer a unique relation between light and mass from the kinematics of satellite galaxies.

**Key words:** galaxies: haloes — galaxies: kinematics and dynamics — galaxies: fundamental parameters — galaxies: structure — methods: statistical

## 1 INTRODUCTION

According to the current paradigm, the mass of a dark matter halo is believed to strongly influence the process of galaxy formation. Hence, a reliable determination of the masses of dark matter haloes can provide important constraints on the physics of galaxy formation. Numerous methods are available to probe the masses of dark matter haloes, including rotation curves (e.g., Rubin et al. 1982), gravitational lensing, either strong (e.g., Gavazzi et al. 2007) or weak (e.g. Mandelbaum et al. 2006), X-ray emission from the hot intra-cluster medium (e.g., Rykoff et al. 2008), and a combined analysis of clustering and abundances of galaxies (e.g., Yang, Mo, & van den Bosch 2003). In this paper we examine another powerful method, which relies on measuring the kinematics of satellite galaxies in order to infer the mass of the dark matter halo in which they orbit.

In general, a dark matter halo hosts one central galaxy,

located at rest at the center of the halo’s potential well, and a population of satellite galaxies orbiting the halo. The line-of-sight (hereafter los) velocity dispersion of these satellite galaxies reflects the depth of the halo’s potential well, and is thus a measure for the halo’s mass. In the case of rich galaxy clusters, the number of satellite galaxies can be sufficient to properly sample the los velocity distribution of its dark matter halo (Carlberg et al. 1996; Carlberg, Yee & Ellingson 1997). In less massive haloes, however, the number of (detectable) satellite galaxies is generally too small to obtain a reliable measure of the los velocity dispersion. However, under the assumption that central galaxies with similar properties (i.e., luminosity) are hosted by haloes of similar masses, one can stack central galaxies and combine the kinematic information of their associated satellites to improve the statistics. Pioneering efforts in this direction were made by Erickson, Gottesman & Hunter (1987), Zaritsky et al. (1993), Zaritsky & White (1994) and Zaritsky et al. (1997). Although these studies were typically limited to samples of less than 100 satellites, they neverthe-

<sup>\*</sup> International Max Planck Research School fellow  
more@mpia.de

less sufficed to demonstrate the existence of extended dark matter haloes around (spiral) galaxies.

More recently, with the advent of large homogeneous galaxy redshift surveys such as the Sloan Digital Sky Survey (SDSS; York et al. 2000) and the Two degree Field Galaxy Redshift Survey (2dFGRS; Colless et al. 2001), it has become possible to apply this method to much larger samples of satellite galaxies (McKay et al. 2002; Prada et al. 2003; Brainerd & Specian 2003; van den Bosch et al. 2004; Conroy et al. 2007; Becker et al. 2007). These studies all found the los velocity dispersion of satellite galaxies,  $\sigma_{\text{sat}}$ , to increase with the luminosity of the host (central) galaxy,  $L_c$ . This is in agreement with the expectation that more massive haloes host more luminous centrals. In a recent study, Norberg, Frenk, & Cole (2008) have shown that the quantitative discrepancies between these previous studies mainly owe to differences in the criteria used to select central hosts and their satellites. This underscores the necessity for a careful treatment of selection effects in order to extract reliable mass estimates from satellite kinematics.

Except for van den Bosch et al. (2004), all previous studies have been extremely conservative in their selection of hosts and satellites. Consequently, despite the fact that the redshift surveys used contain well in excess of 100,000 galaxies, the final samples only contained about 2000 – 3000 satellite galaxies. This severely limits the statistical accuracy of the velocity dispersion measurements as well as the dynamic range in luminosity of the central galaxies for which halo masses can be inferred. The main motivation for using strict selection criteria is to select only ‘isolated’ systems, with satellites that can be treated as tracer particles (i.e., their mass does not cause significant perturbations in the gravitational potential of their host galaxy). Let  $P(M|L_c)$  denote the conditional probability distribution that a central galaxy of luminosity  $L_c$  resides in a halo of mass  $M$ . If the scatter in  $P(M|L_c)$  is sufficiently small, preferentially selecting ‘isolated’ systems should yield an unbiased estimate of  $\langle M \rangle(L_c)$ , which is the first moment of  $P(M|L_c)$ . However, very little is known about the actual amount of scatter in  $P(M|L_c)$  and different semi-analytical models for galaxy formation make significantly different predictions (see discussion in Norberg et al. 2008). If appreciable, the scatter will severely complicate the interpretation of satellite kinematics, and may even cause a systematic bias (van den Bosch et al. 2004; More et al. 2008). Furthermore, even if the scatter is small, in practice, satellites of central galaxies stacked in finite bins of luminosity are used to measure the kinematics. If the satellite sample is small, one has to resort to relatively large bins in order to have sufficient signal-to-noise. Therefore, even if the distribution  $P(M|L_c)$  is relatively narrow, this still implies mixing the kinematics of haloes spanning a relatively large range in halo masses.

In this paper we demonstrate that whenever the scatter in  $P(M|L_c)$  is non-negligible, the  $\sigma_{\text{sat}}(L_c)$  inferred from the data has to be interpreted with great care. In particular, we demonstrate that there is a degeneracy between the first and second moments of  $P(M|L_c)$ , in that two distributions with different  $\langle M \rangle(L_c)$  and different scatter can give rise to the same  $\sigma_{\text{sat}}(L_c)$ . Therefore, a unique  $\langle M \rangle(L_c)$  cannot be inferred from satellite kinematics without a prior knowledge of the second moment of  $P(M|L_c)$ . However, not all hope is lost. In fact, we demonstrate that by using two different

methods to measure  $\sigma_{\text{sat}}(L_c)$ , one can actually break this degeneracy and thus constrain both the mean and the scatter of  $P(M|L_c)$ . In this paper we introduce the methodology, and present the analytical framework required to interpret the data, taking account of the selection criteria used to identify the central host galaxies and their satellites. In More et al. (2008; hereafter Paper II) we apply this method to the SDSS to infer both the mean and the scatter of  $P(M|L_c)$ , which we show to be in good agreement with the results obtained from clustering and galaxy-galaxy lensing analyses. In addition, in Paper II we demonstrate that (i) the scatter in  $P(M|L_c)$  can not be neglected, especially not at the bright end, and (ii) the strict isolation criteria generally used to select centrals and satellites result in a systematic underestimate of the actual  $\langle M \rangle(L_c)$ .

This paper is organized as follows. In Section 2, we present two different schemes to measure the velocity dispersion, the satellite-weighting scheme and the host-weighting scheme. In Section 3, we present a toy model which serves as a basis for understanding the dependence of velocity dispersion estimates on the different parameters of interest. In Sections 4 and 5 we refine our toy model by including selection effects and by using a realistic halo occupation distribution (HOD) model for the central galaxies. We use these more realistic models to investigate how changes in the halo occupation statistics of central galaxies affect the velocity dispersion of satellite galaxies, and we demonstrate how the combination of satellite-weighting and host-weighting can be used to infer both the mean and the scatter of the mass-luminosity relation. We summarize our findings in Section 6. Throughout this paper  $M$  denotes the halo mass in units of  $h^{-1}M_\odot$ .

## 2 WEIGHTING SCHEMES

In order to estimate dynamical halo masses from satellite kinematics one generally proceeds as follows. Using a sample of satellite galaxies, one determines the distribution  $P(\Delta V)$ , where  $\Delta V$  is the difference in the line-of-sight velocity of a satellite galaxy and its corresponding central host galaxy. The scatter in the distribution  $P(\Delta V)$  (hereafter the velocity dispersion), is then considered to be an estimator of the depth of the potential well in which the satellites orbit, and hence of the halo mass associated with the central. In order to measure the velocity dispersion as a function of central galaxy luminosity,  $\sigma_{\text{sat}}(L_c)$ , with sufficient signal-to-noise, one has to combine the los velocity information of satellites which belong to centrals of the same luminosity,  $L_c$ . This procedure is influenced by two effects, namely *mass-mixing* and *satellite-weighting*, which we now discuss in turn.

Mass-mixing refers to combining the kinematics of satellites within haloes of different masses. The mass-luminosity relation (hereafter MLR) of central galaxies can have an appreciable scatter, i.e., the conditional probability distribution  $P(M|L_c)$  is not guaranteed to be narrow. In this case, the satellites used to measure  $\sigma_{\text{sat}}(L_c)$  reside in halo masses drawn from this distribution, and  $\sigma_{\text{sat}}(L_c)$  has to be interpreted as an average over  $P(M|L_c)$ .

In most studies to date, the technique used to measure  $\sigma_{\text{sat}}(L_c)$  implies satellite weighting. This can be elucidated as follows. Let us assume that one stacks  $N_c$  central galaxies,

and that the  $j^{\text{th}}$  central has  $N_j$  satellites. The total number of satellites  $N_{\text{sat}}$  is given by  $\sum_{j=1}^{N_c} N_j$ . Let  $\Delta V_{ij}$  denote the los velocity difference between the  $i^{\text{th}}$  satellite and its central galaxy  $j$ . The average velocity dispersion of the stacked system,  $\sigma_{\text{sw}}$ , is such that

$$\sigma_{\text{sw}}^2 = \frac{\sum_{j=1}^{N_c} \sum_{i=1}^{N_j} (\Delta V_{ij})^2}{\sum_{j=1}^{N_c} N_j} = \frac{1}{N_{\text{sat}}} \sum_{j=1}^{N_c} N_j \sigma_j^2. \quad (1)$$

Here  $\sigma_j$  is the velocity dispersion in the halo of the  $j^{\text{th}}$  central galaxy. The velocity dispersion measured in this way is clearly a satellite-weighted average of the velocity dispersion  $\sigma_j$  around each central galaxy<sup>1</sup>. Although not necessarily directly using Eq. (1), most previous studies have adopted this satellite-weighting scheme (McKay et al. 2002; Brainerd & Specian 2003; Prada et al. 2003; Norberg et al. 2008).

In principle, the satellite-weighting can be undone by introducing a weight  $w_{ij} = 1/N_j$  for each satellite-central pair in the los velocity distribution (van den Bosch et al. 2004; Conroy et al. 2007). The resulting *host-weighted* average velocity dispersion,  $\sigma_{\text{hw}}$ , is such that

$$\sigma_{\text{hw}}^2 = \frac{\sum_{j=1}^{N_c} \sum_{i=1}^{N_j} w_{ij} (\Delta V_{ij})^2}{\sum_{j=1}^{N_c} \sum_{i=1}^{N_j} w_{ij} N_j} = \frac{1}{N_c} \sum_{j=1}^{N_c} \sigma_j^2, \quad (2)$$

and it gives each halo an equal weight.

Consider a sample of central and satellite galaxies with luminosities  $L > L_{\text{min}}$ . The velocity dispersions in the satellite-weighting and host-weighting schemes can be analytically expressed as follows:

$$\sigma_{\text{sw}}^2(L_c) = \frac{\int_0^\infty P(M|L_c) \langle N_{\text{sat}} \rangle_M \langle \sigma_{\text{sat}}^2 \rangle_M dM}{\int_0^\infty P(M|L_c) \langle N_{\text{sat}} \rangle_M dM}, \quad (3)$$

$$\sigma_{\text{hw}}^2(L_c) = \frac{\int_0^\infty P(M|L_c) \langle \sigma_{\text{sat}}^2 \rangle_M dM}{\int_0^\infty P(M|L_c) dM}. \quad (4)$$

Here  $\langle N_{\text{sat}} \rangle_M$  denotes the average number of satellites with  $L > L_{\text{min}}$  in a halo of mass  $M$ , and  $\langle \sigma_{\text{sat}}^2 \rangle_M$  is the square of the los velocity dispersion of satellites averaged over the entire halo.

Consider a MLR of central galaxies that has no scatter, i.e.  $P(M|L_c) = \delta(M - M_0)$ , where  $M_0$  is the halo mass for a galaxy with luminosity  $L_c$ . In this case both schemes give an equal measure of the velocity dispersion, i.e.,  $\sigma_{\text{sw}}^2 = \sigma_{\text{hw}}^2 = \langle \sigma_{\text{sat}}^2 \rangle_{M_0}$ . Most studies to date have assumed the scatter in  $P(M|L_c)$  to be negligible, and simply inferred an average MLR,  $M_0(L_c)$  using  $\sigma_{\text{sw}}^2(L_c) = \langle \sigma_{\text{sat}}^2 \rangle_{M_0}$  (McKay et al. 2002; Brainerd & Specian 2003; Prada et al. 2003; Norberg et al. 2008). However, as shown in van den Bosch et al. (2004), and as evident from the above equations (3) and (4), whenever the scatter in  $P(M|L_c)$  is non-negligible,  $\sigma_{\text{sw}}^2(L_c)$  and  $\sigma_{\text{hw}}^2(L_c)$  can differ significantly<sup>2</sup> (see also Paper II).

In this paper, we show that ignoring the scatter in the MLR of central galaxies can result in appreciable errors in

the inferred mean relation between mass and luminosity. We show, though, that these problems can be avoided by simultaneously modeling  $\sigma_{\text{sw}}^2(L_c)$  and  $\sigma_{\text{hw}}^2(L_c)$ . In particular, we demonstrate that the ratio of these two quantities can be used to determine the actual scatter in the MLR of central galaxies.

### 3 TOY MODEL

In the previous section, we have shown that both  $\sigma_{\text{sw}}^2(L_c)$  and  $\sigma_{\text{hw}}^2(L_c)$  can be analytically expressed in terms of the probability function,  $P(M|L_c)$ , the satellite occupation,  $\langle N_{\text{sat}} \rangle_M$ , and the kinematics of the satellite galaxies within a halo of mass  $M$  specified by  $\langle \sigma_{\text{sat}}^2 \rangle_M$ . In fact, the inversion of equations (3) and (4) presents an opportunity to constrain  $P(M|L_c)$  using the observable  $\sigma_{\text{sw}}^2$  and  $\sigma_{\text{hw}}^2$ . In this section we use a simple toy model to demonstrate that the combination of  $\sigma_{\text{sw}}^2$  and  $\sigma_{\text{hw}}^2$  can be used to constrain the first two moments (i.e., the mean and the scatter) of  $P(M|L_c)$ .

For convenience, let us assume that  $P(M|L_c)$  is a log-normal distribution

$$P(M|L_c) dM = \frac{1}{\sqrt{2\pi\sigma_{\ln M}^2}} \exp \left[ -\left( \frac{\ln(M/M_0)}{\sqrt{2\sigma_{\ln M}^2}} \right)^2 \right] \frac{dM}{M}. \quad (5)$$

Here  $M_0$  is a characteristic mass scale which obeys

$$\ln M_0 = \int_0^\infty P(M|L_c) \ln M dM = \langle \ln M \rangle, \quad (6)$$

and  $\sigma_{\ln M}^2$  reflects the scatter in halo mass at a fixed central luminosity and is given by

$$\sigma_{\ln M}^2 = \int_0^\infty P(M|L_c) (\ln M - \ln M_0)^2 dM. \quad (7)$$

In addition, let us assume that both  $\langle \sigma_{\text{sat}}^2 \rangle_M$  and  $\langle N_{\text{sat}} \rangle_M$  are simple power laws,

$$\langle N_{\text{sat}} \rangle_M = \tilde{N} \left( \frac{M}{10^{12}} \right)^\alpha, \quad (8)$$

$$\langle \sigma_{\text{sat}}^2 \rangle_M = \tilde{S}^2 \left( \frac{M}{10^{12}} \right)^\beta. \quad (9)$$

with  $\alpha$  and  $\beta$  two constants,  $\tilde{N}$  the average number of satellites in a halo of mass  $10^{12} h^{-1} M_\odot$ , and  $\tilde{S}$  the corresponding los velocity dispersion.

Substituting Eqs. (5), (8) and (9) in Eqs. (3) and (4) yields

$$\sigma_{\text{sw}}^2(L_c) = \tilde{S}^2 \left( \frac{M_0}{10^{12}} \right)^\beta \exp \left[ \frac{\sigma_{\ln M}^2 \beta^2}{2} \left( 1 + 2 \frac{\alpha}{\beta} \right) \right], \quad (10)$$

$$\sigma_{\text{hw}}^2(L_c) = \tilde{S}^2 \left( \frac{M_0}{10^{12}} \right)^\beta \exp \left[ \frac{\sigma_{\ln M}^2 \beta^2}{2} \right]. \quad (11)$$

The velocity dispersions  $\sigma_{\text{sw}}(L_c)$  and  $\sigma_{\text{hw}}(L_c)$  depend on both  $M_0$  and  $\sigma_{\ln M}$ , elucidating the degeneracy between the mean mass  $M_0(L_c)$  and the scatter  $\sigma_{\ln M}(L_c)$  of the distribution  $P(M|L_c)$ . In particular, if only  $\sigma_{\text{sw}}(L_c)$  or  $\sigma_{\text{hw}}(L_c)$  is measured, one cannot deduce  $M_0(L_c)$  without having an independent knowledge of the scatter  $\sigma_{\ln M}(L_c)$ . However, the latter can be inferred from the *ratio* of the satellite-weighted to the host-weighted velocity dispersion. In particular, in the case of our toy model,

<sup>1</sup> Note that the velocity dispersion is always averaged in quadrature.

<sup>2</sup> Note that  $\sigma_{\text{sw}}^2 \neq \sigma_{\text{hw}}^2$  is a sufficient but not a necessary condition to indicate the presence of scatter in  $P(M|L_c)$ ; after all, if  $\langle N_{\text{sat}} \rangle_M$  does not depend on mass then  $\sigma_{\text{sw}}^2 = \sigma_{\text{hw}}^2$  independent of the amount of scatter.

$$\sigma_{\ln M}^2 = \frac{1}{\alpha\beta} \ln \left( \frac{\sigma_{\text{sw}}^2}{\sigma_{\text{hw}}^2} \right) \quad (12)$$

Thus, by measuring *both*  $\sigma_{\text{sw}}(L_c)$  and  $\sigma_{\text{hw}}(L_c)$  one can determine both  $M_0(L_c)$  and its scatter  $\sigma_{\ln M}(L_c)$ , provided that the constants  $\alpha$  and  $\beta$  are known. Since virialized dark matter haloes all have the same average density within their virial radii,  $\beta = 2/3$  (e.g. Klypin et al. 1999; van den Bosch et al. 2004). Previous studies have obtained constraints on  $\alpha$  that cover the range  $0.7 \lesssim \alpha \lesssim 1.1$  (e.g. Yang et al. 2005; van den Bosch et al. 2007; Tinker et al. 2007; Yang et al. 2007). Since  $\sigma_{\ln M}^2 \propto \alpha^{-1}$ , this uncertainty directly translates into an uncertainty of the inferred scatter. Therefore, in Paper II, we do not use the constraints on  $\alpha$  available in the literature to infer the mean and scatter of the MLR from real data. Instead, we treat  $\alpha$  as a free parameter and use the average number of observed satellites as a function of the luminosity of central as an additional constraint.

#### 4 SELECTION EFFECTS

The toy model presented in the previous section illustrates that measurements of the satellite-weighted and host-weighted kinematics of satellite galaxies can be used to infer the mean and scatter of the MLR of central galaxies,  $P(M|L_c)$ . However, in practice one first needs a method to select central galaxies and satellites from a galaxy redshift survey. In general, central galaxies are selected to be the brightest galaxy in some cylindrical volume in redshift space, and satellite galaxies are defined as those galaxies that are fainter than the central by a certain amount and located within a cylindrical volume centered on the central. In this section we show how these selection criteria impact on  $\sigma_{\text{sw}}^2$  and  $\sigma_{\text{hw}}^2$ , and how this can be accounted for in the analysis.

No selection criterion is perfect, and some galaxies will be selected as centrals, while in reality they are satellites (hereafter ‘false centrals’). In addition, some galaxies will be selected as satellites of a certain central, while in reality they do not reside in the same halo as the central (hereafter ‘interlopers’). The selection criteria have to be tuned in order to minimize the impact of these false centrals and interlopers. Here we make the assumption that interlopers can be corrected for, and that the impact of false centrals is negligible. Using mock galaxy redshift surveys, van den Bosch et al. (2004) have shown that one can devise adaptive, iterative selection criteria that justify these assumptions (see also Paper II). Here we focus on the impact of these iterative selection criteria on the satellite kinematics in the absence of interlopers and false centrals. Our analytical treatment for selection effects follows the one presented in van den Bosch et al. (2004) except for the inclusion of an extra selection effect. For completeness, we outline this treatment below.

In general, satellite galaxies are selected to lie within a cylindrical volume centered on its central galaxy, and specified by  $R_p < R_s$  and  $|\Delta V| < (\Delta V)_s$ . Here  $R_p$  is the physical separation from the central galaxy projected on the sky and  $\Delta V$  is the los velocity difference between a satellite and its central. Usually,  $(\Delta V)_s$  is chosen sufficiently large,

so that it does not exclude true satellites from being selected. However, in the adaptive, iterative selection criteria of van den Bosch et al. (2004), which we will use in our companion paper II, the aperture radius is tuned so that  $R_s \simeq 0.375 r_{\text{vir}}$ , where  $r_{\text{vir}}$  is the virial radius of the dark matter halo hosting the central-satellite pair. This means that  $\langle N_{\text{sat}} \rangle_M$  and  $\langle \sigma_{\text{sat}}^2 \rangle_M$  in Eqs. (3) and (4) need to be replaced by  $\langle N_{\text{sat}} \rangle_{\text{ap},M}$  and  $\langle \sigma_{\text{sat}}^2 \rangle_{\text{ap},M}$ , respectively. Here  $\langle N_{\text{sat}} \rangle_{\text{ap},M}$  is the average number of satellites in a halo of mass  $M$  that lie within the aperture, and  $\langle \sigma_{\text{sat}}^2 \rangle_{\text{ap},M}$  is the square of the los velocity dispersion of satellite galaxies averaged over the aperture.

The number of satellites present within the aperture,  $\langle N_{\text{sat}} \rangle_{\text{ap},M}$ , is related to the number of satellites given by the halo occupation statistics,  $\langle N_{\text{sat}} \rangle_M$ , via

$$\langle N_{\text{sat}} \rangle_{\text{ap},M} = \begin{cases} f_{\text{cut}} \langle N_{\text{sat}} \rangle_M & \text{if } R_s < r_{\text{vir}} \\ \langle N_{\text{sat}} \rangle_M & \text{if } R_s \geq r_{\text{vir}} \end{cases} \quad (13)$$

with

$$f_{\text{cut}} = \frac{4\pi}{\langle N_{\text{sat}} \rangle_M} \int_0^{R_s} R dR \int_R^{r_{\text{vir}}} n_{\text{sat}}(r|M) \frac{r dr}{\sqrt{r^2 - R^2}}. \quad (14)$$

Here  $n_{\text{sat}}(r|M)$  is the number density distribution of satellites within a halo of mass  $M$ , which is normalized so that

$$\langle N_{\text{sat}} \rangle_M = 4\pi \int_0^{r_{\text{vir}}} n_{\text{sat}}(r|M) r^2 dr. \quad (15)$$

Under the assumption that the satellites are in virial equilibrium within the dark matter halo, and that the velocity dispersion of satellite galaxies within a given halo is isotropic, the los velocity dispersion of satellites within the cylindrical aperture of radius  $R_s$  is given by

$$\langle \sigma_{\text{sat}}^2 \rangle_{\text{ap},M} = \frac{4\pi}{\langle N_{\text{sat}} \rangle_{\text{ap},M}} \int_0^{R_s} dR R \int_R^{r_{\text{vir}}} n_{\text{sat}}(r|M) \sigma_{\text{sat}}^2(r|M) \frac{r dr}{\sqrt{r^2 - R^2}}. \quad (16)$$

Here  $\sigma_{\text{sat}}(r|M)$  is the local, one-dimensional velocity dispersion which is related to the potential  $\Psi$  of the dark matter halo via the Jeans equation

$$\sigma_{\text{sat}}^2(r|M) = \frac{1}{n_{\text{sat}}(r|M)} \int_r^\infty n_{\text{sat}}(r'|M) \frac{\partial \Psi}{\partial r'}(r'|M) dr'. \quad (17)$$

The radial derivative of the potential  $\Psi$  represents the radial force and is given by

$$\frac{\partial \Psi}{\partial r}(r|M) = \frac{4\pi G}{r^2} \int_0^r \rho(r'|M) r'^2 dr', \quad (18)$$

with  $\rho(r|M)$  the density distribution of a dark matter halo of mass  $M$ . The assumptions of virial equilibrium and orbital isotropy are supported by results from numerical simulations which show that dark matter subhaloes (and hence satellite galaxies) are in a steady state equilibrium within the halo and that their orbits are nearly isotropic at least in the central regions (Diemand, Moore, & Stadel 2004). Furthermore, van den Bosch et al. (2004) have demonstrated that anisotropy has a negligible impact on the average velocity dispersion within the selection aperture.

Finally, there is one other effect of the selection criteria to be accounted for which has not been considered in van den Bosch et al. (2004). When selecting central-satellite

pairs, only those centrals are selected with at least one satellite inside the search aperture. This has an impact on the host-weighted velocity dispersions that needs to be accounted for. The probability that a halo of mass  $M$ , which on average hosts  $\langle N_{\text{sat}} \rangle_{\text{ap},M}$  satellites within the aperture  $R_s$ , has  $N_{\text{sat}} \geq 1$  satellites within the aperture, is given by

$$\begin{aligned} P(N_{\text{sat}} \geq 1) &= 1 - P(N_{\text{sat}} = 0) \\ &= 1 - \exp[-\langle N_{\text{sat}} \rangle_{\text{ap},M}] \\ &\equiv \mathcal{P}(\langle N_{\text{sat}} \rangle_{\text{ap},M}). \end{aligned} \quad (19)$$

Here, for the second equality, we have assumed Poisson statistics for the satellite occupation numbers. Note that, in the satellite-weighting scheme, haloes that have zero satellites, by definition, get zero weight. Therefore only the host-weighted velocity dispersions need to be corrected for this effect.

Thus, in light of the selection effects, Eqs. (3) and (4) become

$$\sigma_{\text{sw}}^2(L_c) = \frac{\int_0^\infty P(M|L_c) \langle N_{\text{sat}} \rangle_{\text{ap},M} \langle \sigma_{\text{sat}}^2 \rangle_{\text{ap},M} dM}{\int_0^\infty P(M|L_c) \langle N_{\text{sat}} \rangle_{\text{ap},M} dM}, \quad (20)$$

and

$$\sigma_{\text{hw}}^2(L_c) = \frac{\int_0^\infty P(M|L_c) \mathcal{P}(\langle N_{\text{sat}} \rangle_{\text{ap},M}) \langle \sigma_{\text{sat}}^2 \rangle_{\text{ap},M} dM}{\int_0^\infty P(M|L_c) \mathcal{P}(\langle N_{\text{sat}} \rangle_{\text{ap},M}) dM}. \quad (21)$$

Note that  $\mathcal{P}(\langle N_{\text{sat}} \rangle_{\text{ap},M}) \simeq \langle N_{\text{sat}} \rangle_{\text{ap},M}$  when  $\langle N_{\text{sat}} \rangle_{\text{ap},M} \rightarrow 0$ . This implies that  $|\sigma_{\text{sw}} - \sigma_{\text{hw}}| \rightarrow 0$  for faint centrals (i.e. when  $L_c$  becomes comparable to the luminosity limit of the survey).

## 5 MORE REALISTIC MODELS

Using the methodology described above, we now illustrate how satellite kinematics can be used to constrain the mean and the scatter of the MLR of central galaxies,  $P(M|L_c)$ . We improve upon the toy model described in Section 3 by considering a realistic model for the halo occupation statistics and take the impact of selection criteria into account.

As is evident from the discussion in the previous section, calculating  $\sigma_{\text{sw}}^2(L_c)$  and  $\sigma_{\text{hw}}^2(L_c)$  requires the following input:

- the density distributions of dark matter haloes,  $\rho(r|M)$
- the number density distribution of satellites,  $n_{\text{sat}}(r|M)$
- the halo occupation statistics of centrals,  $P(M|L_c)$ .

We assume that dark matter haloes follow the NFW (Navarro, Frenk, & White 1997) density distribution

$$\rho(r|M) = \frac{M}{4\pi r_s^3 \mu(c)} \left( \frac{r}{r_s} \right)^{-1} \left( 1 + \frac{r}{r_s} \right)^{-2}. \quad (22)$$

Here,  $r_s$  is a characteristic scale radius,  $c = r_{\text{vir}}/r_s$  is the halo's concentration parameter, and

$$\mu(x) \equiv \ln(1+x) - \frac{x}{1+x}. \quad (23)$$

Throughout we use the relation between  $c$  and  $M$  given by Macciò et al. (2007).

We assume that satellite galaxies are spatially unbiased with respect to the dark matter particles, so that their number density distribution is given by Eq. (22) with  $M$  replaced by  $\langle N_{\text{sat}} \rangle_M$ . Note that this is a fairly simplistic assumption.

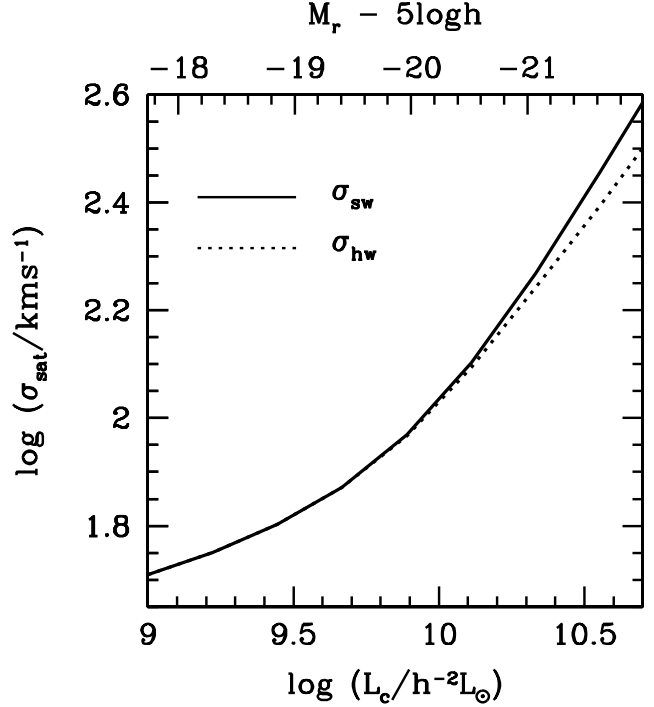


**Figure 1.** The satellite-weighted ( $\sigma_{\text{sw}}$ ) and host-weighted ( $\sigma_{\text{hw}}$ ) velocity dispersions of satellite galaxies for model G1. Note that  $\sigma_{\text{sw}}(L_c) > \sigma_{\text{hw}}(L_c)$  at the bright end, indicating that the MLR of central galaxies,  $P(M|L_c)$ , has a non-negligible amount of scatter.

We address the issue of potential spatial antibias of satellite galaxies in Paper II.

Substituting  $\rho(r|M)$  and  $n_{\text{sat}}(r|M)$  in Eqs. (18) and (17) gives

$$\sigma_{\text{sat}}^2(r|M) = \frac{c V_{\text{vir}}^2}{\mu(c)} \left( \frac{r}{r_s} \right) \left( 1 + \frac{r}{r_s} \right)^2 \int_{r/r_s}^\infty \frac{\mu(x) dx}{x^3 (1+x)^2}, \quad (24)$$

where  $V_{\text{vir}} = (GM/r_{\text{vir}})^{1/2}$  is the circular velocity at  $r_{\text{vir}}$ .

The final ingredient is a realistic model for the halo occupation statistics of centrals and satellites. To that extent, we use the conditional luminosity function (CLF) presented in Cacciato et al. (2008). The CLF, denoted by  $\Phi(L|M)dL$ , specifies the average number of galaxies with luminosities in the range  $L \pm dL/2$  that reside in a halo of mass  $M$ , and is explicitly written as the sum of the contributions due to central and satellite galaxies, i.e.  $\Phi(L|M) = \Phi_c(L|M) + \Phi_s(L|M)$ . From this CLF, the probability distribution  $P(M|L_c)$  follows from Bayes' theorem according to

$$P(M|L_c) = \frac{\Phi_c(L_c|M) n(M)}{\int_0^\infty \Phi_c(L_c|M) n(M) dM}, \quad (25)$$

with  $n(M)$  the halo mass function, while the average number of satellites with  $L \geq L_{\text{min}}$  in a halo of mass  $M$  is given by

$$\langle N_{\text{sat}} \rangle_M = \int_{L_{\text{min}}}^\infty \Phi_s(L|M) dL. \quad (26)$$

The parametric forms for  $\Phi_c(L|M)$  and  $\Phi_s(L|M)$  are motivated by the results of Yang, Mo & van den Bosch (2008, hereafter YMB08), who determined the CLF from the SDSS group catalogue of Yang et al. (2007). In particular,  $\Phi_c(L|M)$  is assumed to follow a log-normal distribution

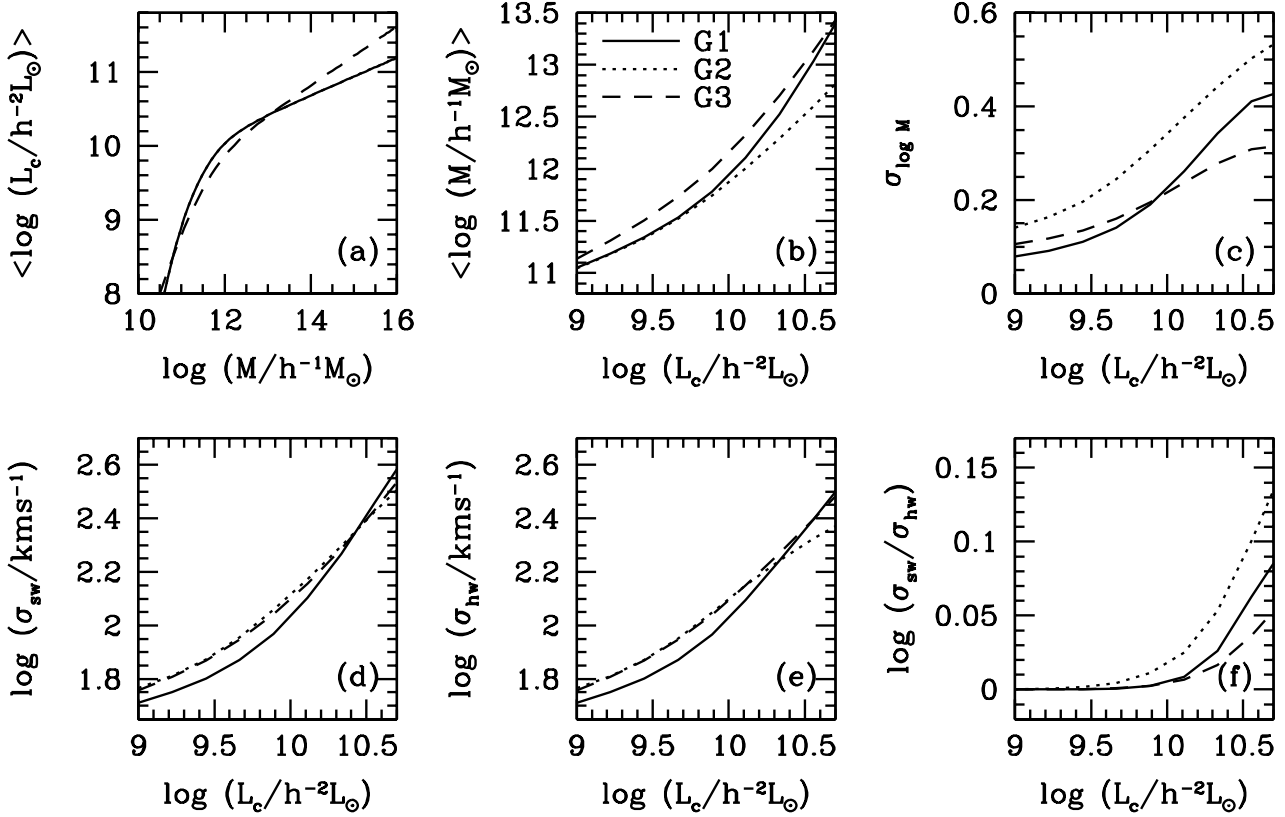


**Figure 2.** Comparison of three models with different HODs for the central galaxies. In all panels the solid line corresponds to model G1, the dotted line to model G2 and the dashed line to model G3 (see Table 1 for the parameters). Panels (a), (b) and (c) show  $\langle \log L_c \rangle(M)$ ,  $\langle \log M \rangle(L_c)$  and  $\sigma_{\log M}(L_c)$ , respectively. Panels (d) and (e) show the predicted satellite-weighted and host-weighted velocity dispersions as function of luminosity, and panel (f) shows the logarithm of the ratio between  $\sigma_{\text{sw}}$  and  $\sigma_{\text{hw}}$ . See text for a detailed discussion.

**Table 1.** Different models for the HOD of centrals

Model	$\sigma_{\log L}$	$\gamma_1$	$\gamma_2$	$L_0$	$M_1$
G1	0.14	3.27	0.25	9.94	11.07
G2	0.25	3.27	0.25	9.94	11.07
G3	0.14	1.80	0.40	9.80	11.46

Three different models describing the MLR of centrals used to predict  $\sigma_{\text{sw}}(L_c)$  and  $\sigma_{\text{hw}}(L_c)$ .

$$\Phi_c(L|M)dL = \frac{\log e}{\sqrt{2\pi}\sigma_{\log L}} \exp\left(-\left[\frac{\log(L/L_c^*)}{\sqrt{2}\sigma_{\log L}}\right]^2\right) \frac{dL}{L}, \quad (27)$$

with  $\sigma_{\log L}$  a free parameter that we take to be independent of halo mass, and

$$L_c^*(M) = L_0 \frac{(M/M_1)^{\gamma_1}}{[1 + (M/M_1)^{\gamma_1 - \gamma_2}]} \quad (28)$$

which has four additional free parameters: two slopes,  $\gamma_1$  and  $\gamma_2$ , a characteristic halo mass,  $M_1$ , and a normalization,  $L_0$ . Note that,  $L_c^* \propto M^{\gamma_1}$  for  $M \ll M_1$  and  $L_c^* \propto M^{\gamma_2}$  for  $M \gg M_1$ . Cacciato et al. (2008) constrained the free parameters,  $\sigma_{\log L}$ ,  $\gamma_1$ ,  $\gamma_2$ ,  $M_1$  and  $L_0$ , by fitting the SDSS luminosity function of Blanton et al. (2003) and the galaxy-galaxy correlation lengths as a function of luminosity from Wang et al. (2007). The resulting best-fit parameters are listed in the first row of Table 1, and constitute our fidu-

cial model G1. We also consider two alternative models for  $\Phi_c(L|M)$ , called G2 and G3, the parameters of which are also listed in Table 1. For  $\Phi_s(L|M)$  we adopt the model of Cacciato et al. (2008) throughout, without any modifications: i.e. models G1, G2, and G3 only differ in  $P(M|L_c)$  and have the same  $n_{\text{sat}}(r|M)$ .

Having specified all necessary ingredients, we now compute the satellite weighted and host-weighted satellite kinematics for our fiducial model G1 using Eqs. (20) and (21). The results are shown as solid and dotted lines in Fig. 1, where we have adopted a minimum satellite luminosity of  $L_{\text{min}} = 10^9 h^{-2} L_\odot$ . At the faint-end, the velocity dispersions  $\sigma_{\text{sw}}$  and  $\sigma_{\text{hw}}$  are equal, this simply reflects the fact that  $\langle N_{\text{sat}} \rangle_M \rightarrow 0$  if  $L_c \rightarrow L_{\text{min}}$ . At the bright end, though, the non-zero scatter in  $P(M|L_c)$  causes the difference between  $\sigma_{\text{sw}}$  and  $\sigma_{\text{hw}}$  to increase systematically with increasing  $L_c$ . This is a generic trend for any realistic halo occupation model (see also van den Bosch et al. 2004).

The upper panels of Fig. 2 show the mean and scatter of the MLR of central galaxies in models G1 (solid lines), G2 (dotted lines) and G3 (dashed lines). Panel (a) plots  $\langle \log L_c \rangle(M) = \log(L_c^*)$ , which reveals the double power-law behavior of Eq. (28), panel (b) shows the inverse relation,

$$\langle \log M \rangle(L_c) = \int_0^\infty P(M|L_c) \log M dM. \quad (29)$$

and panel (c) shows the scatter in the MLR,  $\sigma_{\log M}(L_c)$ , deduced by using

$$\sigma_{\log M}^2 = \int_0^\infty P(M|L_c) [\log M - \langle \log M \rangle(L_c)]^2 dM. \quad (30)$$

Note that  $\sigma_{\log M}(L_c)$  increases with increasing  $L_c$ , even though the scatter  $\sigma_{\log L}$  is constant with halo mass. This simply owes to the fact that the slope of  $\langle \log L_c \rangle(M)$  becomes shallower with increasing  $L_c$ , as illustrated in Fig. 3.

The comparison between models G1 and G2 illustrates the effect of changing the scatter  $\sigma_{\log L}$  in  $\Phi_c(L|M)$ . Both models have exactly the same  $\langle \log L_c \rangle(M)$  (the solid line overlaps the dotted line in panel a). However, because the scatter  $\sigma_{\log L}$  in G2 is larger than in G1 (see Table 1), the  $\langle \log M \rangle(L_c)$  of G2 is significantly lower than that of G1 at the bright end ( $\sim 0.5$  dex at the bright end). This is due to the shape of the halo mass function. Increasing the scatter adds both low mass and high mass haloes to the distribution  $P(M|L_c)$  (cf. Eqs. [25] and [29]), and the overall change in the average halo mass depends on the slope of the halo mass function. Brighter galaxies live on average in more massive haloes where the halo mass function is steeper. In particular, when the halo mass range sampled by  $P(M|L_c)$  lies in the exponential tail of the halo mass function, an increase in the scatter adds many more low mass haloes than massive haloes, causing a shift in the average halo mass towards lower values. On the other hand, fainter galaxies live in less massive haloes, where the slope of the halo mass function is much shallower. Consequently, a change in the scatter does not cause an appreciable change in the average mass. Finally, as expected, the scatter in the MLR,  $\sigma_{\log M}(L_c)$ , in G2 is higher than for G1 at all luminosities (see panel c).

Panels (d) and (e) of Fig. 2 show the analytical predictions for  $\sigma_{\text{sw}}(L_c)$  and  $\sigma_{\text{hw}}(L_c)$ , respectively. Note that models G1 and G2 predict satellite kinematics that are significantly different (which can be distinguished given the typical measurement errors in Paper II), even though both have exactly the same  $\langle \log L_c \rangle(M)$ . In particular, model G2 predicts larger  $\sigma_{\text{sw}}$  and  $\sigma_{\text{hw}}$  at the faint end, but lower  $\sigma_{\text{sw}}$  and  $\sigma_{\text{hw}}$  at the bright end. The trend at the faint is due to the fact that the scatter  $\sigma_{\log M}(L_c)$  is higher in G2 than in G1. Quantitatively, this is evident from Eqs. (10) and (11), which demonstrate that both the satellite weighted and host weighted satellite kinematics increase with increasing scatter. At the bright end, however, the drastic decrease in  $\langle \log M \rangle(L_c)$  for G2 with respect to G1 overwhelms this boost and causes  $\sigma_{\text{sw}}$  and  $\sigma_{\text{hw}}$  to be lower in G2.

Now consider model G3. This model has the same amount of scatter as model G1, but we have tuned its parameters ( $\gamma_1, \gamma_2, M_1, L_0$ ) that describe  $\langle \log L_c \rangle(M)$  such that its  $\sigma_{\text{sw}}(L_c)$  closely matches that of model G2 (the dotted and dashed curves in panel (d) are almost overlapping). As is evident from panels (a)-(c), though, the MLR of G3 is very different from that of G2. Note that the higher values of  $\langle \log M \rangle(L_c)$  for G3 are compensated by its lower values of  $\sigma_{\log M}(L_c)$ , such that the satellite-weighted kinematics are virtually identical. This clearly illustrates the degeneracy between the mean and the scatter of the MLR: One can decrease the mean of the MLR and yet achieve the same  $\sigma_{\text{sw}}$  by increasing the scatter of the MLR. It also shows that  $\sigma_{\text{sw}}$  alone does not yield sufficient information to uniquely constrain the MLR.

Note, though, that although  $\sigma_{\text{sw}}$  is the same for models G2 and G3, their host-weighted satellite kinematics,

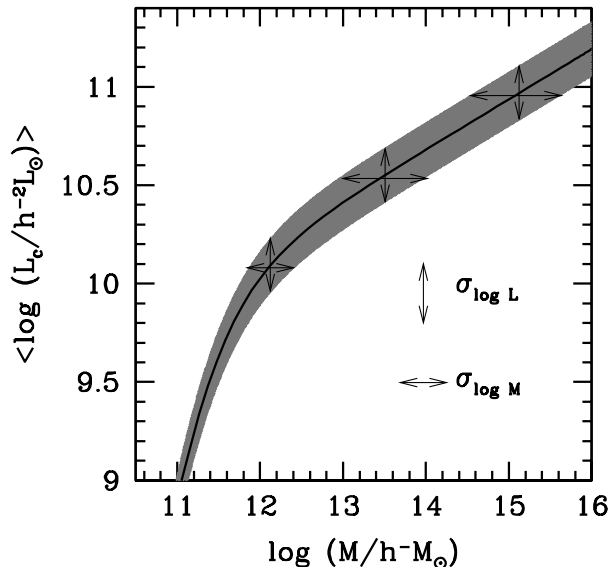


**Figure 3.** Illustration of the MLR of central galaxies. The solid black line indicates the mean of the  $L_c$ - $M$  relation, while the gray scale region reflects the scatter. In this particular case the scatter in  $P(L_c|M)$  (indicated by vertical arrows) is taken to be constant with halo mass. Note, though, that the scatter in  $P(M|L_c)$  (indicated by horizontal arrows) increases with increasing  $L_c$ ; this simply is due to the fact that the slope of the mean  $L_c$ - $M$  relation becomes shallower with increasing halo mass.

$\sigma_{\text{hw}}(L_c)$ , are different at the bright end. In fact, the ratios  $\sigma_{\text{sw}}/\sigma_{\text{hw}}$  for models G2 and G3 are clearly different. The logarithm of this ratio, shown in panel (f), follows the same trend as  $\sigma_{\log M}(L_c)$ , i.e. it is higher for model G2 than for G3. This is in agreement with our toy model, according to which the ratio  $\sigma_{\text{sw}}/\sigma_{\text{hw}}$  increases with the scatter  $\sigma_{\log M}(L_c)$  (cf. Eq. [12]). This illustrates once again that the combination of  $\sigma_{\text{sw}}$  and  $\sigma_{\text{hw}}$  allows one to constrain both the mean and the scatter of the MLR simultaneously.

## 6 SUMMARY

The kinematics of satellite galaxies is a powerful probe of the masses of the dark matter haloes surrounding central galaxies. With the advent of large, homogeneous redshift surveys, it has become possible to probe the mass-luminosity relation (MLR) of central galaxies spanning a significant range in luminosities. Unfortunately, since most centrals only host a few satellite galaxies with luminosities above the flux limit of the redshift survey, one generally needs to stack a large number of central galaxies within a given luminosity bin and combine the velocity information of their satellites. Because of the finite bin-width, and because the MLR has intrinsic scatter, this stacking results in combining the kinematics of satellite galaxies in haloes of different masses, which complicates the interpretation of the data. Unfortunately, most previous studies have ignored this issue, and made the oversimplified assumption that the scatter is negligible.

Using realistic models for the halo occupation statistics, and taking account of selection effects, we have demonstrated a degeneracy between the mean and the scatter of the MLR: one can change the mean relation between halo

mass,  $M$ , and central galaxy luminosity,  $L_c$ , and simultaneously change the scatter around that mean relation, such that the observed satellite kinematics,  $\langle\sigma_{\text{sat}}\rangle(L_c)$ , are unaffected.

We have also presented a new technique to break this degeneracy, based on measuring the satellite kinematics using two different weighting schemes: host-weighting (each central galaxy gets the same weight) and satellite weighting (each central galaxy gets a weight proportional to its number of satellites). In general, for central galaxies close to the magnitude limit of the survey, the average number of satellites per host is close to zero, and the satellite-weighted velocity dispersion,  $\sigma_{\text{sw}}$ , is equal to the host-weighted velocity dispersion,  $\sigma_{\text{hw}}$ . This is because only those centrals with at least one satellite are used to measure the satellite kinematics. For brighter centrals, however,  $\sigma_{\text{sw}} > \sigma_{\text{hw}}$  and the actual ratio of these two values is larger for MLRs with more scatter (see Eq. [12] and panels c and f of Fig. 2). Hence, the combination of  $\sigma_{\text{sw}}(L_c)$  and  $\sigma_{\text{hw}}(L_c)$  contains sufficient information to constrain both the mean and the scatter of the MLR of central galaxies. In our companion paper (More et al. 2008), we apply this method to the SDSS, and show that the amount of scatter inferred from the data is in excellent agreement with other, independent constraints. In the companion paper, we also address the issues of measurement errors, sampling effects and interlopers.

In a recent study, Becker et al. (2007) analyzed the kinematics of MaxBCG clusters (Koester et al. 2007) and inferred the mean and the scatter of the mass-richness relation (here richness is a measure for the number of galaxies that reside in the cluster). Becker et al. combined the kinematics of satellite galaxies in finite bins of cluster richness and measured the second and fourth moments of the host-weighted velocity distribution. They used these two moments simultaneously to determine the mean and the scatter of the mass-richness relation. This method is complementary to that presented here, and it will be interesting to compare both methods and investigate their relative strengths and weaknesses. We intend to address this in a future study.

Finally we emphasize that the scatter in the conditional probability function  $P(M|L_c)$  is expected to increase with increasing  $L_c$ . This is due to the fact that the slope of  $\langle L_c \rangle(M)$ , which is the mean of  $P(L_c|M)$ , becomes shallower with increasing halo mass. Hence, when stacking haloes according to the luminosity of the central galaxy, one cannot ignore the scatter in  $M$ , even when the scatter in  $P(L_c|M)$  is small. This has important implications for any technique that relies on stacking, such as satellite kinematics and galaxy-galaxy lensing (see e.g. Tasitsiomi 2004; Cacciato et al. 2008)

## ACKNOWLEDGMENTS

We are grateful to Kris Blindert, Anupreeta More, and Peder Norberg for valuable discussion.

## REFERENCES

- Brainerd T. G., Specian M. A., 2003, *ApJ*, 593, L7  
Cacciato M., van den Bosch F. C., More S., Li R., Mo H. J., Yang X., 2008, *MNRAS*, submitted  
Carlberg R. G., Yee H. K. C., Ellingson E., Abraham R., Gravel P., Morris S., Pritchett C. J., 1996, *ApJ*, 462, 32  
Carlberg R. G., Yee H. K. C., Ellingson E., 1997, *ApJ*, 478, 462  
Colless M., et al., 2001, *MNRAS*, 328, 1039  
Conroy C., et al., 2007, *ApJ*, 654, 153  
Diemand J., Moore B., Stadel J., 2004, *MNRAS*, 352, 535  
Erickson L. K., Gottesman S. T., Hunter J. H., Jr., 1987, *Nat*, 325, 779  
Gavazzi R., Treu T., Rhodes J. D., Koopmans L. V. E., Bolton A. S., Burles S., Massey R. J., Moustakas L. A., 2007, *ApJ*, 667, 176  
Klypin A., Gottlöber S., Kravtsov A. V., Khokhlov A. M., 1999, *ApJ*, 516, 530  
Koester B. P., et al., 2007, *ApJ*, 660, 239  
Kravtsov A. V., Berlind A. A., Wechsler R. H., Klypin A. A., Gottlöber S., Allgood B., Primack J. R., 2004, *ApJ*, 609, 35  
Macciò A. V., Dutton A. A., van den Bosch F. C., Moore B., Potter D., Stadel J., 2007, *MNRAS*, 378, 55  
Mandelbaum R., Seljak U., Kauffmann G., Hirata C. M., Brinkmann J., 2006, *MNRAS*, 368, 715  
McKay T. A., et al., 2002, *ApJ*, 571, L85  
More S., van den Bosch F. C., Cacciato M., 2008, *MNRAS*, submitted, arXiv:0807.4532  
Navarro J. F., Frenk C. S., White S. D. M., 1997, *ApJ*, 490, 493  
Norberg P., Frenk C. S., Cole S., 2008, *MNRAS*, 383, 646  
Prada F., et al., 2003, *ApJ*, 598, 260  
Rubin V. C., Ford W. K., Jr., Thonnard N., Burstein D., 1982, *ApJ*, 261, 439  
Rykoff E. S., et al., 2008, *ApJ*, 675, 1106  
Tasitsiomi A., Kravtsov A. V., Wechsler R. H., Primack J. R., 2004, *ApJ*, 614, 533  
Tinker J. L., Norberg P., Weinberg D. H., Warren M. S., 2007, *ApJ*, 659, 877  
van den Bosch F. C., Norberg P., Mo H. J., Yang X., 2004, *MNRAS*, 352, 1302  
van den Bosch F. C., et al., 2007, *MNRAS*, 376, 841  
Wang Y., Yang X., Mo H. J., van den Bosch F. C., Weinmann S. M., Chu Y., 2007, preprint (arXiv:0711.4431)  
Yang X., Mo H. J., van den Bosch F. C., 2003, *MNRAS*, 339, 1057  
Yang X., Mo H. J., Jing Y. P., van den Bosch F. C., 2005, *MNRAS*, 358, 217  
Yang X., Mo H. J., van den Bosch F. C., Pasquali A., Li C., Barden M., 2007, *ApJ*, 671, 153  
Yang X., Mo H. J., van den Bosch F. C., 2008, *ApJ*, 676, 248  
York D. G., et al., 2000, *AJ*, 120, 1579  
Zaritsky D., Smith R., Frenk C., White S. D. M., 1997, *ApJ*, 478, 39  
Zaritsky D., Smith R., Frenk C., White S. D. M., 1993, *ApJ*, 405, 464  
Zaritsky D., White S. D. M., 1994, *ApJ*, 435, 599